Endocytosis-dependent lysosomal degradation of Src induced by protease-activated receptor 1

Chung-Che Tsai[1], Fang-Ting Kuo[1], Sung-Bau Lee[2,3], Yu-Ting Chang[1] and Hua-Wen Fu[1,2] (iD)

1 Institute of Molecular and Cellular Biology, National Tsing Hua University, Hsinchu, Taiwan, Republic of China
2 Department of Life Science, National Tsing Hua University, Hsinchu, Taiwan, Republic of China
3 College of Pharmacy, Taipei Medical University, Taiwan, Republic of China

Correspondence
H.-W. Fu, Institute of Molecular and Cellular Biology, National Tsing Hua University, 101, Sec. 2, Kuang-Fu Rd, Hsinchu, 30013 Taiwan, Republic of China
Tel: +886 3 5742485
E-mail: hwfu@life.nthu.edu.tw

Src plays a critical role in regulating cellular responses induced by protease-activated receptor 1 (PAR1). Here, we found that PAR1 activation induces lysosomal degradation of Src. Src is associated and trafficked together with activated PAR1 to early endosomes and then sorted to lysosomes for degradation. Blocking agonist-induced endocytosis of PAR1 by inhibition of dynamin activity suppresses PAR1-induced degradation of Src. However, Src activity is neither required for agonist-induced PAR1 internalization nor required for Src degradation upon PAR1 activation. We show that PAR1 activation triggers endocytosis-dependent lysosomal degradation of Src in both human embryonic kidney 293 and human umbilical vein endothelial cells. Our finding provides a new paradigm for how an irreversibly activated receptor regulates its downstream signalling.

Keywords: endocytosis; lysosomal degradation; PAR1; Src

Thrombin, a multifunctional serine protease generated at sites of vascular injury, plays a critical role in hemostasis and thrombosis. This protease also induces inflammatory and proliferative responses in a variety of cells [1–3]. The cellular responses induced by thrombin are mainly mediated by protease-activated receptor 1 (PAR1), a G protein-coupled receptor (GPCR). Thrombin cleaves the N-terminal exodomain of PAR1 to unmask a new N-terminus beginning with the sequence, SFLLRN [4]. The newly exposed N-terminus then serves as a tethered ligand, binding intramolecularly to the receptor to trigger transmembrane signalling [5].

Synthetic peptides that mimic this tethered ligand act as the agonists of PAR1 and activate the receptor independently of thrombin and proteolysis [4,6,7]. Activated-PAR1 couples to the members of the Gαi/o, Gαq/11 and Gα12/13 protein families, which in turn regulate a variety of intracellular effectors [8]. The desensitization of PAR1 is regulated by G protein-coupled receptor kinase (GRK)-mediated phosphorylation and binding of β-arrestins [9–12]. β-arrestin 1 but not β-arrestin 2 is predominantly responsible for PAR1 desensitization [11]. Upon exposure to thrombin, the cleaved, activated PAR1 is rapidly internalized

and sorted mainly to lysosomes [13,14]. Due to the irreversible activation of PAR1, lysosomal sorting of PAR1 is critical for the termination of receptor signalling [15]. That is the reason why the trafficking behaviour of PAR1 is distinct from those of most other well-studied GPCRs, which are recycled to the plasma membrane after agonist-dependent internalization.

Similar to other GPCRs, agonist-induced internalization of PAR1 is clathrin- and dynamin-dependent [16]. However, β-arrestins that function as endocytic adaptor proteins for GPCR are not required for agonist-induced internalization of PAR1 and its subsequent degradation [11,17]. After PAR1 activation, β-arrestin 1 and β-arrestin 2 are recruited to the activated receptor to form the complexes containing Src and extracellular signal-regulated kinase 1/2 (ERK1/2) [17]. β-arrestin 1 increases Src activity to promote PAR1-induced phosphorylation of ERK1/2, whereas β-arrestin 2 blocks Src activation to reduce PAR1-induced phosphorylation of ERK1/2 [17]. In addition to mediate ERK activation, β-arrestin 1 promotes a rapid Src-dependent activation of Akt induced by PAR1 [18]. In contrast, β-arrestin 2 appears to promote PAR1-induced degradation of Src [17]. Even though both β-arrestins serve as adaptor proteins to regulate PAR1 signalling, β-arrestin 1 initiates and β-arrestin 2 terminates Src-dependent signalling induced by PAR1.

Src, a nonreceptor tyrosine kinase downstream of GPCR, mediates a number of cell responses, including proliferation, survival, adhesion and migration [19,20]. The activation and deactivation of Src are regulated by its two tyrosine phosphorylation sites. The phosphorylation of tyrosine 419 (Tyr419) residue in the catalytic domain of Src stabilizes the active conformation to enhance its kinase activity, whereas phosphorylation of tyrosine 530 (Tyr530) residue at the C-terminal regulatory segment of Src induces the intramolecular interaction between the phosphorylated Tyr530 residue and its Src-homology 2 (SH2) domain of Src to inhibit its kinase activity [21]. The activation of Src by GPCRs can be mediated by G proteins and β-arrestins. Heterotrimic Gαs and Gαi proteins directly bind to the catalytic domain of Src and change its conformation, leading to increased accessibility of Src to its substrates [22]. β-arrestin 1 interacts with the SH3 domain and the N-terminal region of the catalytic domain of Src to disrupt the intramolecular interactions of Src, resulting in the activation of Src [23,24]. For termination of Src-mediated signalling, active Src can be deactivated by phosphorylation at its Tyr530 residue by C-terminal Src tyrosine kinase (Csk) or degraded *via* a ubiquitin-proteasome

system-dependent mechanism [25,26]. It has been reported that PAR1-induced Src activation is attenuated by Csk, which is recruited by phoshocaveolin-1 to downregulate the Src kinase activity after PAR1 activation [27]. Alternatively, the activation of PAR1 induces degradation of Src to terminate its signalling [17]. However, it is unclear how Src is degraded after PAR1 activation.

Src is a critical signal transducer of PAR1-mediated cellular responses such as proliferation, angiogenesis and inflammation [28–31]. Upon PAR1 activation, Src is recruited from the cytosol to the receptor at the cell membrane by β-arrestins [17]. Given the fact that PAR1 is sorted to lysosomes and degraded, we hypothesize that Src is trafficked with activated PAR1 and sorted to lysosomes for degradation. In this study, we first investigated whether PAR1-induced degradation of Src is lysosome-dependent. We then examined whether endocytosis of PAR1 is involved in PAR1-mediated degradation of Src. Finally, we explored whether Src activity is required for PAR1 endocytosis-dependent degradation of Src.

Materials and methods

Reagents

Synthetic peptide SFLLRN-NH$_2$ was synthesized by Syn-Pep Crop. (Dublin, CA, USA). Chloroquine, poly-L-lysine (molecular weight: 70 000–150 000), gelatin, and bovine serum albumin (BSA) were purchased from Sigma (St. Louis, MO, USA). PP1 and dynasore were purchased from Biomol (Plymouth Meeting, PA, USA) and Abmole BioScience (Houston, TX, USA), respectively.

Cell culture

Human embryonic kidney 293 (HEK293) cells stably expressing FLAG-tagged PAR1 [17] were cultured in Eagle's minimum essential medium (MEM)/Earle's salts (Invitrogen, Carlsbad, CA, USA) supplemented with 10% fetal bovine serum (FBS) (Hyclone Laboratories, Logan, UT, USA). Human umbilical vein endothelial cells (HUVECs) were purchased from Bioresource Collection and Research Center (BCRC, Hsinchu, Taiwan) and cultured in Medium 199 (M199) (Invitrogen) supplemented with 10% heat-inactivated FBS, 2 mM L-glutamine, 25 units·mL^{-1} heparin and 30 μg·mL^{-1} endothelial cell growth supplement on T75 flasks pre-coated with 1% gelatin. Both cells were maintained in the presence of 100 units·mL^{-1} penicillin and 100 μg·mL^{-1} streptomycin at 37 °C under 5% CO$_2$ and saturated humidity. HUVECs were used at passages 2–6.

DNA transfection

HEK293 cells stably expressing FLAG-PAR1 were seeded on a 10 cm dish (Nunc, Roskilde, Denmark) and grown to 95% confluence. Cells were transfected with 20 µg of DNA and 40 µL of lipofectamine 2000 (Invitrogen) according to the manufacturer's instructions. The pcDNA3.1 mammalian expression vector containing cDNA encoding N-terminal haemagglutinin (HA)-tagged human dynamin-1 or dynamin-1 mutant K44A [32] or the pEGFP-C mammalian expression vectors expressing N-terminal green fluorescent protein (GFP)-tagged human vacuolar protein sorting 4 (hVps4) or hVps4-E228Q mutant [33] were used for transfection.

Immunofluorescence staining

HEK293 cells stably expressing FLAG-tagged PAR1 were grown on poly-L-Lysine-coated coverslips for 24 h and serum-starved for 1 h. When the cellular trafficking of PAR1 was examined, the cells were preincubated with anti-PAR1 1809 rabbit antiserum at a dilution of 1 : 500 at 4 °C for 1 h and then exposed to 100 µM SFLLRN at 37 °C for various periods of time. The cells were put on ice to stop internalization of PAR1, fixed with 4% paraformaldehyde (PFA) in D-PBS, pH 7.2, for 15 min, and then permeabilized and quenched with D-PBS, pH 7.2, containing 0.5% Triton X-100, 150 mM sodium acetate and 1% BSA at 4 °C for 20 min. The cells were washed once with ice-cold D-PBS, pH 7.2, and incubated with either anti-Src monoclonal antibody or anti-LAMP1 antibody at a dilution of 1 : 200 in D-PBS, pH 7.2, containing 1% BSA at 4 °C for 2 h or incubated with anti-Rab5 antibody at a concentration of 2.5 µg·mL^{-1} at room temperature for 1 h. The cells were then washed three times with D-PBS, pH 7.2, containing 1% BSA, for 5 min each time. After incubation with the species-appropriate fluorescence-conjugated secondary antibodies at a concentration of 2.5 µg·mL^{-1} in D-PBS, pH 7.2, containing 1% BSA at 4 °C for 2 h in dark, the cells were washed five times with D-PBS, pH 7.2, and mounted with prolong antifade mounting kit (Molecular Probe, Eugene, OR, USA). When PAR1-induced co-localization of Src and LAMP1 was examined, the experimental procedure is the same except that the cells were not preincubated with the antibody against PAR1 and were incubated with both anti-Src polyclonal antibody and anti-LAMP1 antibody at a dilution of 1 : 200 in D-PBS, pH 7.2, containing 1% BSA at 4 °C for 2 h after permeabilization. For analysis of co-localization of PAR1 and clathrin on the plasma membrane patches, the experimental procedure is essentially the same as previous described [16] except that PAR1 was detected by anti-PAR1 1809 antiserum and clathrin was detected by the mouse monoclonal anti-clathrin heavy chain antibody. The details of the antibodies were listed in Table 1. Images were collected using a Zeiss Axioskop2 LSM5 Pascal confocal microscopy fitted with a Plan-Neofluar 100x/N.A. 1.30 objective.

Immunoblotting

Cells were lysed in the modified radioimmunoprecipitation assay lysis (RIPA) buffer containing 10 mM Tris-HCl, pH 7.4, 150 mM NaCl, 0.05% SDS, 1% Nonidet P-40, 0.5 mM ethylenediaminetetraacetic acid (EDTA), 0.2 mM phenylmethylsulfonyl fluoride (PMSF), 1 µg·mL^{-1} aprotinin, 4 µM leupeptin, 1 µM pepstatin A, 1 mM Na$_3$VO$_4$ and 1 mM NaF. The cell suspension was sonicated 30 times with 50% amplitude and 0.5 cycle on ice using an UP50H ultrasonic processor (Dr. Hielscher, Berlin, Germany). Protein concentrations were determined by the Bradford method (Bio-Rad protein Assay, Bio-Rad Laboratory, Hercules, CA, USA). Cell lysates were then mixed with 4X SDS sample buffer and heated at 65 °C for 10 min to detect FLAG-tagged PAR1 or at 95 °C for 10 min to detect other proteins. The protein samples were separated on a 9% SDS–polyacrylamide gel and then transferred to polyvinylidene difluoride (PVDF) membrane (Pall Corporation, Cortland, NY, USA). Immunoblotting was performed essentially the same as previously described [34] except that the primary antibodies listed in Table 1 for immunoblotting were used. The signal of the protein of interest was visualized by an enhanced chemiluminescence (ECL) substrate (PerkinElmer, Norwalk, CT, USA) expected that the signal of endogenous PAR1 was visualized by Immobilon Western Chemiluminescent HRP substrate (Millipore, Bedford, MA, USA). The bands were imaged by LAS-3000 imaging system (Fujifilm, Tokyo, Japan) and quantified using densitometry by MULTIGAUGE software version 3.0 (Fujifilm).

Internalization assay

Internalization assay was performed using a cell-based enzyme-linked immunosorbent assay (ELISA) similarly as previously described [27] with some modifications. HEK293 cells stably expressing FLAG-tagged PAR1 were seeded on a 24-well plate (Falcon, Franklin Lakes, NJ, USA), which was precoated with poly-L-lysine, and grown to 95% confluence. HUVECs were seeded on a 24-well plate precoated with 1% gelatin. The cells were serum-starved for 1 h unless specified and then left unstimulated or stimulated with 100 µM SFLLRN at 37 °C for the indicated times. The cells were fixed with 4% PFA in D-PBS at 4 °C for 10 min and washed with the ice-cold HEPES-buffered medium for three times. The HEPES-buffered medium used for HEK293 cells is composed of MEM Earle's Salts supplemented with 20 mM HEPES, pH 7.4, 1 mg·mL^{-1} BSA, and 1 mM CaCl$_2$ and the HEPES-buffered medium used for HUVECs is composed of M199 supplemented with 20 mM HEPES, pH 7.4, 2% heat-inactivated FBS, and 1 mg·mL^{-1}

Table 1. Antibodies used in this study.

Name of the antibody	Clonality	Host	Clone	Catalog number	Concentration or dilution factor	Source
Anti-PAR1 1809 rabbit antiserum	Antiserum	Rabbit	N/A	N/A	1 : 500[a]	Dr. Shaun R. Coughlin, University of California, USA [50]
Clathrin heavy chain	Monoclonal	Mouse	N/A	610499	2.5 µg·mL^{-1a}	BD Biosciences, San Diego, CA, USA
ERK1/2	Antiserum	Rabbit	N/A	M5670	1 : 3000[b]	Sigma, St Louis, MO, USA
FLAG tag	Monoclonal	Mouse	M1	F-3040	2 µg·mL$^{-1b,c}$	Sigma, St Louis, MO, USA
Fluorescein-conjugated goat anti-mouse IgG (H+L)	Polyclonal	Goat	N/A	115-095-003	1 : 400[a]	Jackson ImmunoResearch, West Grove, PA, USA
Fluorescein-conjugated goat anti-rabbit IgG (H+L)	Polyclonal	Goat	N/A	111-095-144	1 : 400[a]	Jackson ImmunoResearch, West Grove, PA, USA
GFP	Monoclonal	Mouse	3D8A1B8	Gm0001-02	1 : 1000[b]	Abking Biotechnologies, Taipei, Taiwan
HA tag	Monoclonal	Mouse	12CA5	1666606	1 µg·mL^{-1b}	Roche Molecular Biochemicals, Basel, Swiss
IgG from mouse serum	Purified IgG	Mouse	N/A	I5381	2 µg·mL^{-1c}	Sigma, St Louis, MO, USA
LAMP1	Monoclonal	Mouse	H5G11	sc-18821	1 : 200[a]	Santa Cruz Biotechnology, Santa Cruz, CA, USA
PAR1	Monoclonal	Mouse	ATAP2	sc-13503	1 : 1000[b], 2 µg·mL^{-1c}	Santa Cruz Biotechnology, Santa Cruz, CA, USA
Peroxidase-conjugated goat anti-mouse IgG (H+L)	Polyclonal	Goat	N/A	115-035-003	1 : 5000[b,c]	Jackson ImmunoResearch, West Grove, PA, USA
Peroxidase-conjugated goat anti-rabbit IgG (H+L)	Polyclonal	Goat	N/A	111-035-003	1 : 5000[b]	Jackson ImmunoResearch, West Grove, PA, USA
Phospho-ERK1/2	Monoclonal	Mouse	E-4	sc-7383	1 : 3000[b]	Santa Cruz Biotechnology, Santa Cruz, CA, USA
Phospho-Src family (Tyr416)	Polyclonal	Rabbit	N/A	2101	1 : 1000[b]	Cell Signaling, Beverly, MA, USA
Rab5	Monoclonal	Mouse	N/A	610725	2.5 µg·mL^{-1a}	BD Biosciences, San Diego, CA, USA
Rhodamine-conjugated goat anti-mouse IgG (H+L)	Polyclonal	Goat	N/A	115-025-146	1 : 400[a]	Jackson ImmunoResearch, West Grove, PA, USA
Rhodamine-conjugated goat anti-rabbit IgG (H+L)	Polyclonal	Goat	N/A	111-025-144	1 : 400[a]	Jackson ImmunoResearch, West Grove, PA, USA
Src	Monoclonal	Mouse	GD11	05-184	1 : 500[b]	Millipore, Bedford, MA, USA
Src	Polyclonal	Rabbit	N/A	2108	1 : 200[a]	Cell Signaling, Beverly, MA, USA
Tubulin-α	Monoclonal	Mouse	DM1A	MS-581-P	1 : 5000[b]	NeoMarker, Fremont, CA, USA

N/A, not available. [a]Immunofluorescence staining. [b]Immunoblotting. [c]Internalization assay.

BSA. HEK293 cells were incubated with anti-FLAG M1 antibody (Sigma) and HUVECs were incubated with anti-PAR1 antibody (Santa Cruz, Santa Cruz, CA, USA) and its corresponding mouse IgG antibody (Sigma) at a concentration of 2 µg·mL^{-1} in the HEPES-buffered medium at room temperature for 60 min. The cells were washed with the HEPES-buffered medium for three times and then incubated with horseradish peroxidase-conjugated goat anti-mouse secondary antibody (Jackson ImmunoResearch, West Grove, PA, USA) at a dilution of 1 : 5000 in the HEPES-buffered medium at room temperature for 1 h. After being washed with D-PBS for three times, the cells were incubated with 250 µL of 1-Step ABTS (2, 2′-azino-bis-3-ethylbenzthiazoline-6-sulfonic acid, Pierce, Rockford, IL, USA) for 30 min to detect the amount of bound horseradish peroxidase-conjugated goat anti-mouse secondary antibody on the cell surface. Aliquots of 200 µL were then transferred into the wells of a 96-well plate and the optical density was measured at 405 nm using a microplate spectrophotometer (Bio-Rad Model 550).

Statistics analysis

Statistical significance compared with control was determined by a paired two-tailed Student's *t*-test using Excel 2010 (Microsoft, Roselle, IL, USA). All data are presented

as mean ± standard deviation (SD). Statistical significance was defined as $P < 0.05$.

Results

PAR1-induced lysosome-dependent degradation of Src

Upon PAR1 activation, Src is recruited to the receptor by β-arrestins to form a signalling complex [17]. To investigate how Src signalling transduced from this PAR1 complex is terminated, we first monitored agonist-induced intracellular trafficking of PAR1 and Src in HEK293 cells stably expressing FLAG-tagged PAR1 by confocal microscopy. In unstimulated cells, PAR1 was located at the cell surface and Src was distributed both at the plasma membrane and in the cytosol (Fig. 1A). After 15 min of stimulation with a PAR1-specific peptide agonist, SFLLRN, PAR1 was internalized into the cells as the green puncta (Fig. 1A). Of interest, Src, shown as the red puncta, was co-localized with PAR1 (Fig. 1A). Meanwhile, internalized PAR1 was co-localized with Rab5, an early endosome marker (Fig. 1A). This result indicates that Src is associated and trafficked together with PAR1 to early endosomes after SFLLRN stimulation. We next examined whether both Src and PAR1 are then sorted to lysosomes. After 30 min of SFLLRN stimulation, PAR1 and Src, which are shown as green puncta, were both co-localized with lysosome-associated membrane protein 1 (LAMP1), shown as red puncta (Fig. 1B). These results indicate that Src is trafficked with activated PAR1 and both of them are sorted to lysosomes.
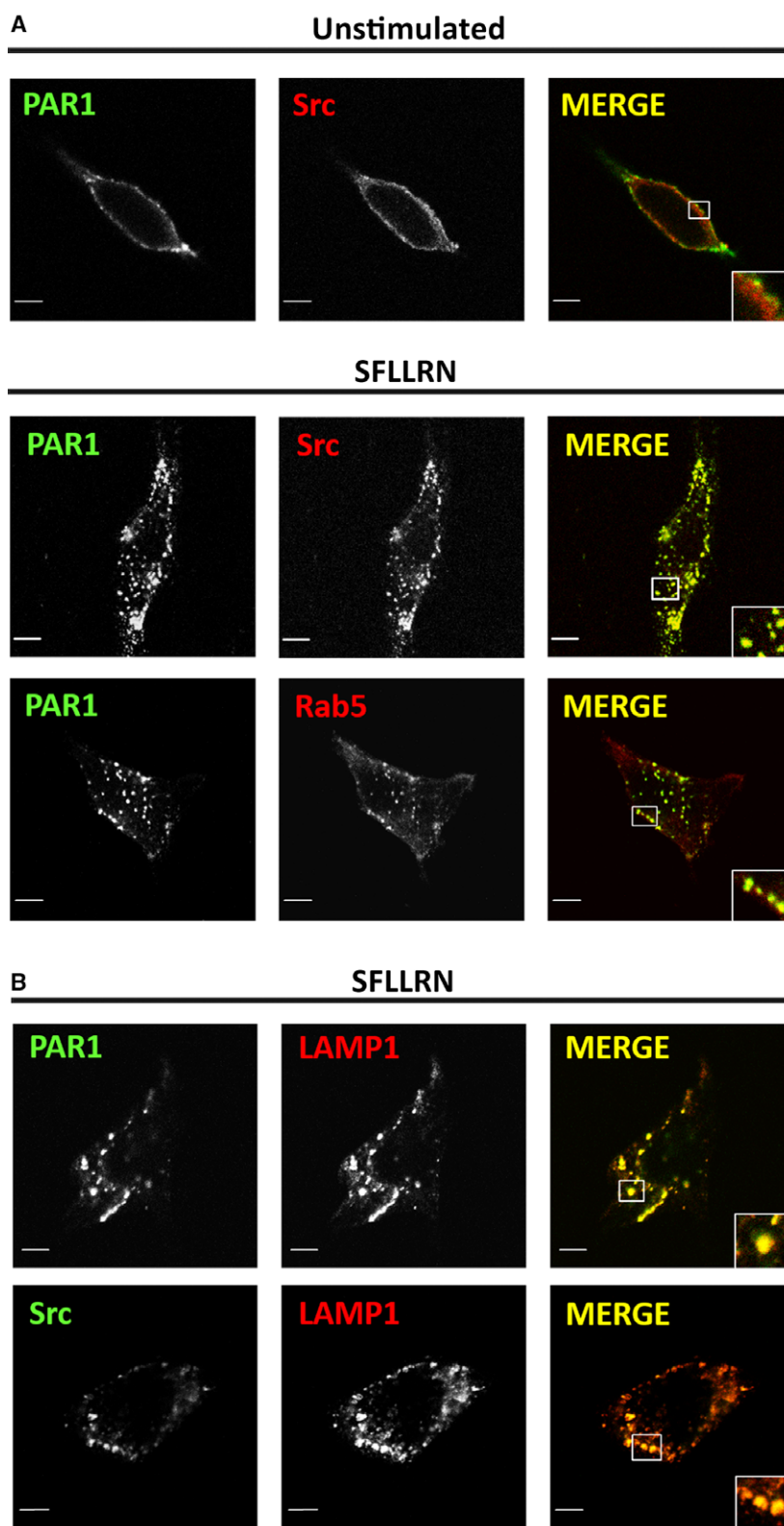
Since activation of PAR1 induces the degradation of Src [17], whether Src is trafficked with activated PAR1 to lysosomes for degradation was examined by monitoring PAR1-induced degradation of Src in HEK293 cells stably expressing FLAG-tagged PAR1 in the presence and absence of chloroquine, a lysosomal inhibitor. Treatment of the cells with SFLLRN resulted in a time-dependent degradation of Src and FLAG-tagged PAR1 (Fig. 2A). After 2 h of SFLLRN stimulation, the amount of Src was decreased by almost 39% (Fig. 2A). In cells pretreated with chloroquine, the decrease in the amount of Src and FLAG-tagged PAR1 induced by SFLLRN was inhibited (Fig. 2A). It has been reported that Vps4 mediates multivesicular body (MVB) sorting of PAR1 [35]. To further support that Src is trafficked to MVB/lysosome for degradation after PAR1 activation, we examined whether overexpression of dominant-negative Vps4-E228Q mutant inhibits PAR1-induced degradation of Src. In cells transfected with wild-type Vps4 and the control

vector, the amount of Src and FLAG-tagged PAR1 gradually decreased at 1 and 2 h after SFLLRN stimulation (Fig. 2B). In cells transfected with dominant-negative Vps4-E228Q mutant, the decrease in the amount of Src and FLAG-tagged PAR1 induced by SFLLRN was inhibited (Fig. 2B). These results indicate that PAR1-induced degradation of Src is lysosome-dependent in HEK293 cells.

We speculated that PAR1-induced lysosomal degradation of Src is required for the termination of Src-dependent signalling induced by PAR1. To test this hypothesis, we examined whether inhibition of PAR1-induced degradation of Src by chloroquine increases PAR1-induced activation of Src. The activation of PAR1 by SFLLRN for 5–120 min induced a biphasic phosphorylation of Tyr419 of Src with the first peak at 5 min and second peak at 60 min (Fig. 2C). Treatment of chloroquine did increase the phosphorylation level of Src induced by PAR1 (Fig. 2C). We next examined whether chloroquine treatment increases the activation of ERK1/2 induced by PAR1. The rationale to choose ERK1/2 is that Src is the main upstream molecule of ERK1/2 in HEK293 cells upon PAR1 activation [17]. The activation of PAR1 by SFLLRN also induced a biphasic phosphorylation of ERK1/2 with the first peak at 5 min and second peak at 60 min (Fig. 2C). After SFLLRN stimulation for 120 min, the expression of ERK1/2 is decreased (Fig. 2C). However, chloroquine treatment significantly increased the phosphorylation level of ERK1/2 in response to SFLLRN stimulation at 15 and 30 min and inhibited the decrease in ERK1/2 expression induced by SFLLRN stimulation (Fig. 2C). We also found that treatment of the cells with PP1 significantly inhibited the phosphorylation of ERK1/2 after SFLLRN stimulation for 5–30 min (Fig. S1). These results indicate that inhibition of lysosomal degradation of Src by chloroquine prolongs the first peak of ERK1/2 activation induce by PAR1. Thus, PAR1-induced lysosomal degradation of Src may be specific for termination of PAR1-mediated endosomal Src signalling.

PAR1 endocytosis-dependent degradation of Src

Upon receptor activation, PAR1 was co-localized with clathrin at the plasma membrane in HEK293 cells (Fig. S2), which is consistent with the previous findings that agonist-induced endocytosis of PAR1 is mediated by clathrin [15,27]. It has also been reported that activated PAR1 is internalized in a dynamin-dependent manner in HeLa cells [16]. To investigate whether PAR1-induced degradation of Src depends on the
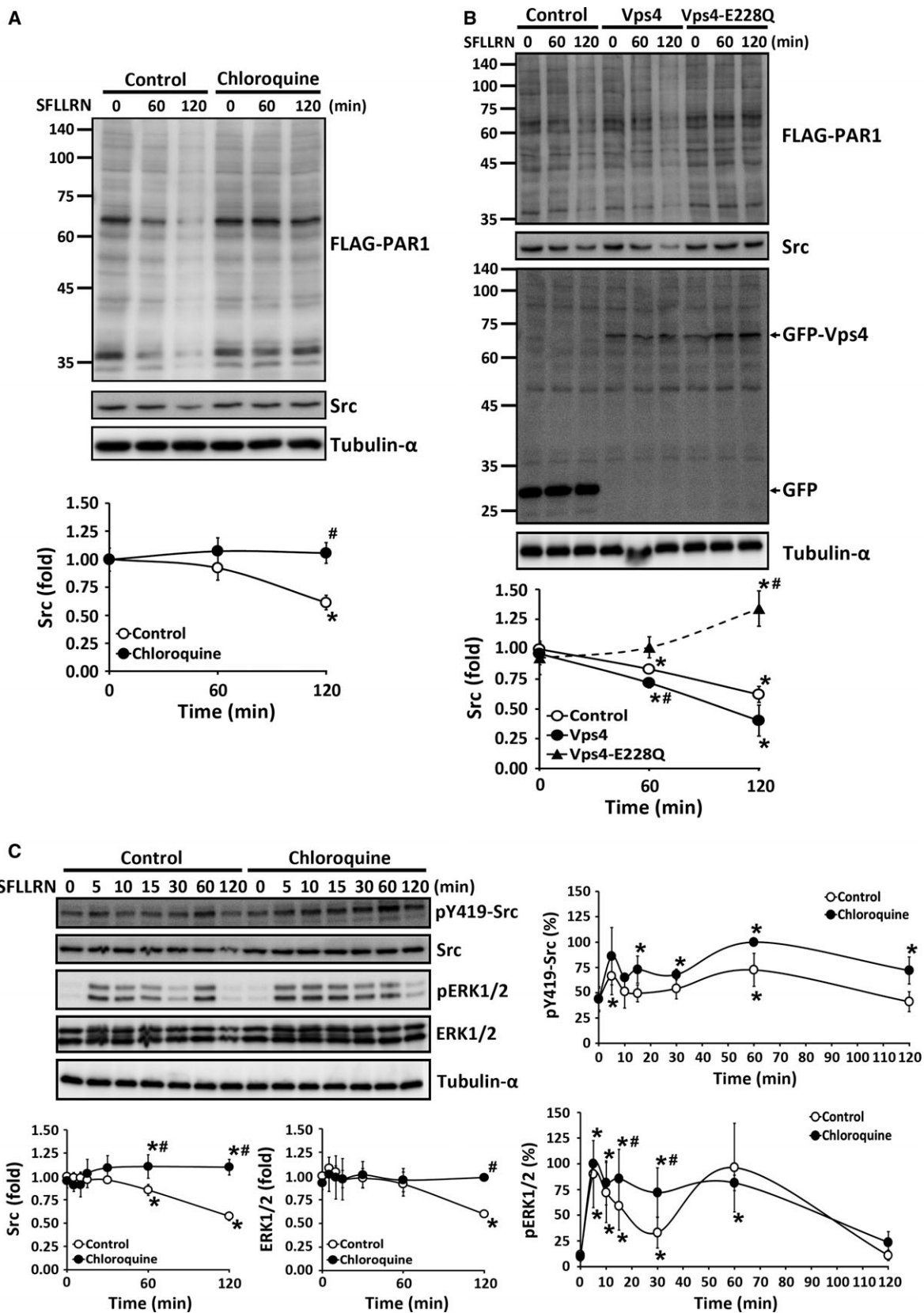
Fig. 1. Activated PAR1 co-localizes with Src in early endosomes and lysosomes. HEK293 cells stably expressing FLAG-tagged PAR1 were serum-starved for 1 h. (A) Serum-starved cells were preincubated with anti-PAR1 1809 antiserum at 4 °C for 1 h and then left unstimulated or stimulated with 100 μM SFLLRN for 15 min. The cells were fixed, permeabilized and immunostained with antibodies against Src at 4 °C for 2 h or Rab5, an early endosomal marker, at room temperature for 1 h. Co-localization of FLAG-tagged PAR1 with Src or Rab5 is represented as yellow in the merge images. Scale bar 5 μm. (B) Serum-starved cells were stimulated with 100 μM SFLLRN for 30 min and then incubated with anti-PAR1 1809 antiserum at 4 °C for 1 h. Cells were fixed, permeabilized and immunostained with antibody against Src or LAMP1, a lysosomal marker, at 4 °C for 2 h. Co-localization of LAMP1 with PAR1 or Src is represented as yellow in the merge images. Scale bar 5 μm. Similar results were obtained in three-independent experiments.

Fig. 2. Activation of PAR1 induces lysosomal degradation of Src. (A) HEK293 cells stably expressing FLAG-tagged PAR1 were serum-starved overnight. Serum-starved cells were left un-pretreated (control) or pretreated with 100 μM chloroquine for 1 h and then left unstimulated or stimulated with 100 μM SFLLRN for the indicated times. The cells were lysed and cell lysates were subjected to immunoblotting to detect FLAG-tagged PAR1, Src, and tubulin-α. The results are expressed as fold increase compared to the level in unstimulated control cells and represented as the mean ± SD of five-independent experiments. (B) HEK293 cells stably expressing FLAG-tagged PAR1 were transfected with GFP-tagged Vps4, GFP-tagged dominant-negative Vps4 (Vps4-E228Q), or the pEGFP-C3 control vector. The cells were serum-starved overnight and then left unstimulated or stimulated with 100 μM SFLLRN for the indicated times. Cells were lysed and cell lysates were subjected to immunoblotting to detect FLAG-tagged PAR1, Src, GFP-tagged Vps4 and tubulin-α. The results are expressed as fold increase compared to the level in unstimulated control cells and represented as the mean ± SD of three-independent experiments. (C) HEK293 cells stably expressing FLAG-tagged PAR1 were treated as described in A. The cell lysates were subjected to immunoblotting to detect pY419-Src, Src, pERK1/2, ERK1/2 and tubulin-α. The results are expressed as the percentage of the maximal phosphorylation of Tyr419 of Src obtained at 60 min of stimulation and phosphorylation of ERK1/2 obtained at 5 min of stimulation in cells pretreated with chloroquine for phosphorylated Src and phosphorylated ERK1/2, respectively, and are expressed as fold increase compared to the level in unstimulated control cells for Src and ERK1/2. Data were represented as the mean ± SD of three-independent experiments. (A–C) *$P < 0.05$ vs. unstimulated cells in each group; #$P < 0.05$ vs. the control cells stimulated with SFLLRN at the same time point.

---

endocytosis of activated PAR1, we first determined whether agonist-induced endocytosis of PAR1 is dependent on dynamin in HEK293 cells. In this experiment, HEK293 cells stably expressing FLAG-PAR1 were transiently transfected with the dominant-negative dynamin K44A mutant, which is defective in its GTPase activity [36], to examine its effect on agonist-induced PAR1 internalization. After SFLLRN stimulation for 15 min, the amount of PAR1 remaining on the cell surface was reduced to 26% and 41% in cells transfected with wild-type dynamin and the control vector respectively (Fig. 3A). However, in cells transfected with the dominant-negative dynamin K44A mutant, the stimulation of SFLLRN did not significantly alter the amount of PAR1 on the cell surface (Fig. 3A). Thus, the overexpression of the dominant-negative dynamin K44A mutant inhibits agonist-induced internalization of PAR1 in HEK293 cells. This result indicates that agonist-induced endocytosis of PAR1 is dynamin-dependent in HEK293 cells.

We next overexpressed the dominant-negative dynamin K44A mutant in HEK293 cells stably expressing FLAG-PAR1 to examine the effect of inhibition of agonist-induced PAR1 internalization on PAR1-induced degradation of Src. In cells transfected with wild-type dynamin and the control vector, the amount of Src gradually decreased at 60 and 120 min after SFLLRN stimulation (Fig. 3B). At 120 min stimulation of SFLLRN, the amount of Src was slightly but significantly reduced in cells overexpressing wild-type dynamin than that in cells transfected with the control vector (Fig. 3B). Although overexpression of the dominant-negative dynamin K44A mutant reduced the basal expression of Src in HEK293 cells, the amount of Src did not decrease after SFLLRN stimulation (Fig. 3B). This result indicates that overexpression of the dominant-negative dynamin K44A mutant inhibits

PAR1-induced degradation of Src. Thus, PAR1-induced degradation of Src depends on the endocytosis of activated PAR1. Many endocytic adaptor proteins play a role not only in membrane sorting during endocytosis but also in regulating gene expression [37]. The reduced basal expression of Src in cells overexpressed with dominant-negative dynamin K44A mutant could be due to the inhibition of gene expression of Src caused by the blocking of cellular endocytosis.

No requirement for Src activity in agonist-induced internalization of PAR1 and PAR1 endocytosis-independent degradation of Src

Src-mediated tyrosine phosphorylation of dynamin is required for agonist-induced internalization of β2-adrenergic receptors (β2-AR) [38] and epidermal growth factor receptor (EGFR) [39]. It is possible that Src-mediated tyrosine phosphorylation of dynamin is involved in endocytosis-mediated degradation of Src induced by PAR1. To determine whether Src activity is required for PAR1-induced degradation of Src, we treated HEK293 cells stably expressing FLAG-PAR1 with PP1, a Src kinase inhibitor, to examine its effect on the amount of Src present in this cell upon PAR1 activation. The treatment of the cells with PP1 inhibited SFLLRN-stimulated phosphorylation of Src (Fig. 4A). No significant differences in the amounts of Src were detected in cells with and without the treatment of PP1 after stimulation with SFLLRN (Fig. 4A), suggesting that Src activity is not involved in PAR1-induced degradation of Src. We thus examined whether Src activity is required for agonist-induced internalization of PAR1. The simulation of the cells with SFLLRN caused a time-dependent internalization of PAR1, whereas the treatment of PP1 did not affect SFLLRN-stimulated internalization of
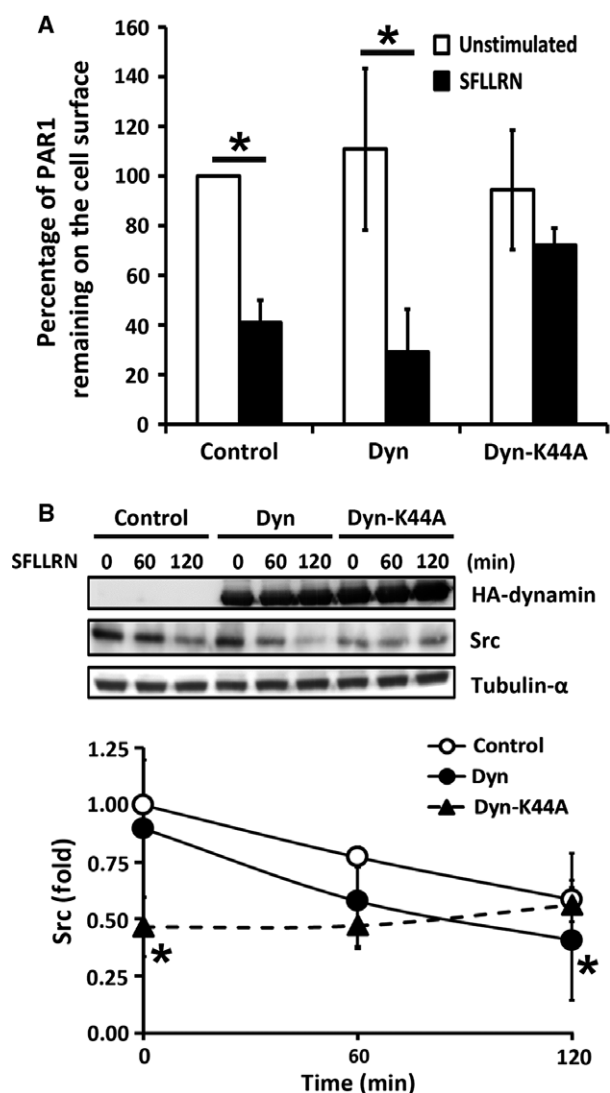
Fig. 3. PAR1-induced Src degradation is mediated by dynamin-dependent receptor endocytosis. HEK293 cells stably expressing FLAG-tagged PAR1 were transfected with HA-tagged dynamin (Dyn), HA-tagged dominant-negative dynamin (Dyn-K44A), and the control vector. The cells were serum-starved overnight. (A) Serum-starved cells were left unstimulated or stimulated with 100 μM SFLLRN for 15 min and then subjected to the internalization assay. The results are expressed as the percentage of PAR1 remaining on the cell surface compared to the level in unstimulated control cells. Data are represented as the mean ± SD of three-independent experiments. *$P < 0.05$ vs. unstimulated cells in each group. (B) Serum-starved cells were left unstimulated or stimulated with 100 μM SFLLRN for the indicated times. The cells were lysed and cell lysates were subjected to immunoblotting to detect HA-tagged dynamin, Src and tubulin-α. The results are expressed as fold increase compared to the level in unstimulated control cells and represented as the mean ± SD of three-independent experiments. *$P < 0.05$ vs. the control cells stimulated with SFLLRN at the same time point.

PAR1 (Fig. 4B). Thus, Src activity is not required for PAR1 endocytosis-dependent degradation of Src. These findings suggest that Src-mediated tyrosine phosphorylation of dynamin is not required for agonist-induced PAR1 internalization.

PAR1-induced lysosomal degradation of Src in HUVECs

To determine whether lysosomal degradation of Src is induced by endogenous PAR1, we examined the effect of chloroquine on the expression of PAR1 and Src in HUVECs after PAR1 activation. The stimulation of HUVECs with SFLLRN resulted in a time-dependent degradation of PAR1 and Src (Fig. 5A). Stimulation with SFLLRN for 120 min led to a marked decrease in the amount of PAR1, whereas the amount of Src was decreased by almost 34% after 180 min of SFLLRN stimulation (Fig. 5A). In cells pretreated with chloroquine, the decrease in the amount of Src and PAR1 induced by SFLLRN was inhibited (Fig. 5A). Thus, PAR1 induces degradation of Src in HUVECs and this degradation is lysosome-dependent. We next examined whether inhibition of PAR1 endocytosis blocks PAR1-induced degradation of Src in HUVECs. After SFLLRN stimulation for 60 min, the amount of PAR1 remaining on the cell surface was increased from 31% to 83% in cells treated with dynasore, an inhibitor of dynamin, as compared to that in the DMSO-treated control cells (Fig. 5B), indicating that agonist-induced endocytosis of PAR1 is dynamin-dependent in HUVECs. Further, SFLLRN-induced degradation of Src and PAR1 in cells pretreated with dynasore was markedly inhibited as compared to that in the control cells (Fig. 5C). These results indicate that blocking of PAR1 endocytosis inhibits PAR1-induced degradation of Src and PAR1 in HUVECs. Thus, receptor endocytosis-dependent lysosomal degradation of Src induced by endogenous PAR1 in HUVECs is consistent with those observed in HEK293 cells.

Discussion

In the present study, we show that PAR1 induces lysosomal degradation of Src. The finding that inhibition of agonist-induced PAR1 internalization by dominant-negative dynamin blocks PAR1-induced degradation of Src further supports the notion that Src is trafficked together with activated PAR1 to the endocytic vesicles and then sorted together with PAR1 to lysosomes for degradation. However, the activity of Src is not required
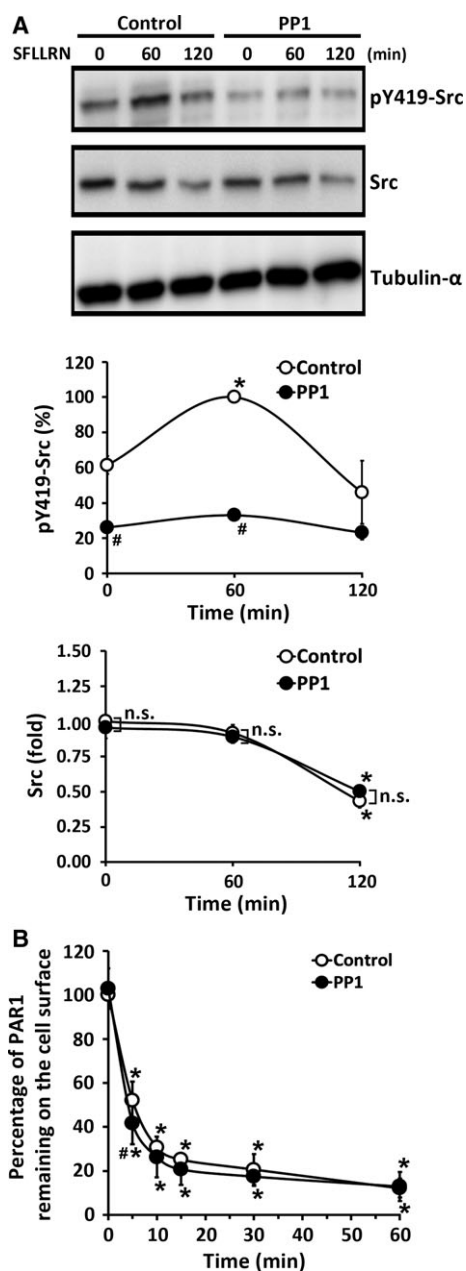
Fig. 4. PAR1-induced Src degradation and receptor internalization are independent of Src activity. HEK293 cells stably expressing FLAG-tagged PAR1 were serum-starved overnight. Serum-starved cells were left un-pretreated (control) or pretreated with 20 μM PP1 for 90 min and then left unstimulated or stimulated with 100 μM SFLLRN for the indicated times. (A) The cells were lysed and cell lysates were subjected to immunoblotting to detect pY419-Src, Src and tubulin-α. The results are expressed as the percentage of the maximal phosphorylation of Tyr419 of Src obtained at 60 min of stimulation in the control cells for phosphorylated Src and are expressed as fold increase compared to the level in unstimulated control cells for Src. Data are represented as the mean ± SD of three-independent experiments. (B) The cells were subjected to the internalization assay. The results are expressed as the percentage of PAR1 remaining on the cell surface compared to the level in unstimulated control cells. Data were represented as the mean ± SD of three-independent experiments. (A, B) *$P < 0.05$ vs. unstimulated cells in each group; #$P < 0.05$ vs. the control cells stimulated with SFLLRN at the same time point; n.s., non-significant.

multivesicular bodies and then to lysosomes for degradation, which is independent of its ubiquitination [35,41]. The lysosomal sorting of PAR1 requires endosomal-sorting complexes required for transport (ESCRT)-III [35]. ESCRT also regulates the endosomal trafficking of Src [42]. It has been suggested that active Src is sorted to the late endosomal-lysosomal compartment in an ESCRT-dependent pathway [43]. In this study, we show that Src is trafficked together with activated PAR1 to endosomes and then to lysosomes for degradation. Also, endocytosis of PAR1 is required for PAR1-induced degradation of Src. These findings, together with the previous findings just mentioned, support the idea that Src is recruited to the activated PAR1 and then sorted together with PAR1 to lysosomes for degradation in an ESCRT-dependent pathway.

Active Src is degraded by a ubiquitin-dependent mechanism [25,26,40]. So far, Cbl-c is the only known escort E3 ubiquitin ligase to mediate lysosomal degradation of active Src [40]. We have previously shown that PAR1-induced degradation of Src is inhibited in cells depleted of β-arrestin-2 [17]. Since β-arrestins function as adapters for multiple E3 ubiquitin ligases to regulate the ubiquitination and trafficking of GPCRs [44], it is possible that β-arrestin-2 serves as an adaptor for an E3 ubiquitin ligase to induce ubiquitination of Src for directing its lysosomal sorting induced by PAR1. However, this possibility awaits further investigation.

It has been reported that Src-mediated phosphorylation of dynamin plays a role in promoting clathrin-mediated

for agonist-induced PAR1 internalization and PAR1-induced degradation of Src. Our findings identify a role of receptor endocytosis in regulation of PAR1 signalling through mediating lysosomal degradation of Src.

Although it has been suggested that active Src undergoes lysosomal degradation [40], the study presented here provides the first evidence that Src is sorted to lysosomes for degradation after PAR1 activation. Upon PAR1 activation, β-arrestins recruit Src and ERK1/2 to form the signalling complexes with PAR1 [17]. To terminate PAR1 signalling, activated PAR1 is sorted to
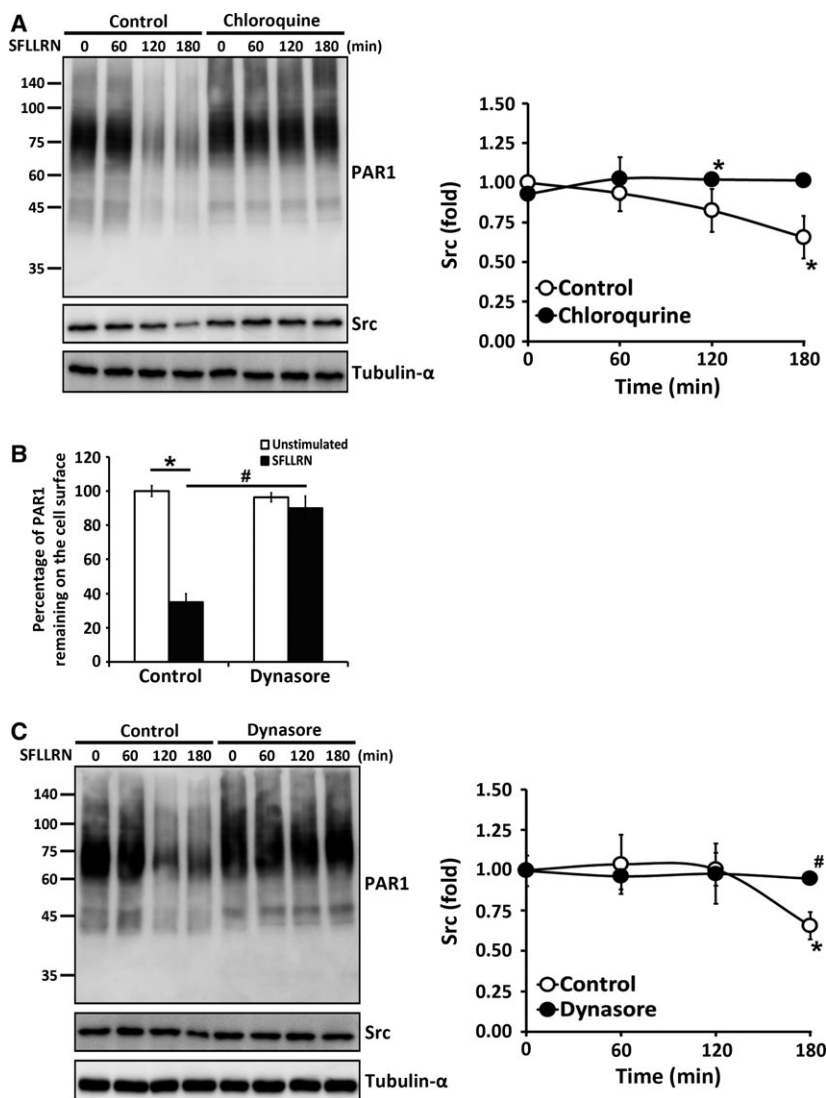
Fig. 5. Activation of PAR1 induces endocytosis-dependent lysosomal degradation of Src in HUVEC cells. HUVECs were serum-starved in M199 supplemented with 2% heat-inactivated FBS for 16 h. The serum-starved cells were pretreated with 100 μM chloroquine (A), 50 μM dynasore (B, C), or DMSO (B, C) at 37 °C for 1 h and then left unstimulated or stimulated with 100 μM SFLLRN at 37 °C for the indicated times (A, C) or 1 h (B). (A, C) The cells were lysed and cell lysates were subjected to immunoblotting to detect PAR1, Src and tubulin-α. The results are expressed as fold increase compared to the level in unstimulated control cells and represented as the mean ± SD of three-independent experiments. (B) The cells were subjected to the internalization assay. The results are expressed as the percentage of PAR1 remaining on the cell surface compared to the level in unstimulated control cells. Data were represented as the mean ± SD of three-independent experiments. (A–C) $*P < 0.05$ vs. unstimulated cells in each group; $^{\#}P < 0.05$ vs. the control cells stimulated with SFLLRN at the same time point.

endocytosis of EGFR, β2-AR and transferrin receptor [38,39,45]. Src also mediates phosphorylation of other endocytic machinery such as clathrin, β2-adaptin and cortactin [45–48]. Agonist-dependent phosphorylation of β2-adaptin mediated by Src is involved in activation of clathrin-dependent endocytosis of several GPCRs [48]. In contrast, dynamin- and clathrin-dependent endocytosis of PAR1 does not require Src activity. This finding indicates that agonist-induced endocytosis of PAR1 does not require Src-mediated phosphorylation of the endocytic machinery. Recently, Src has been implicated in the regulation of postendosomal trafficking through the phosphorylation of Rab7 [49]. Our finding that PAR1 endocytosis-dependent degradation of Src does not require Src activity suggests that Src activity is not involved in the postendocytic sorting of Src to lysosomes induced by PAR1. Since the molecular mechanism of agonist-dependent endocytosis and lysosomal sorting of PAR1 is quite unique as compared to those of other GPCRs, PAR1 endocytosis-dependent lysosomal sorting of Src might be regulated by a different mode from the endocytosis and lysosomal sorting of other GPCRs.

In summary, our findings unveil a new mechanism of how PAR1 induces degradation of Src. We show that PAR1 activation triggers receptor endocytosis-dependent lysosomal degradation of Src. Src is recruited to the activated PAR1 and then sorted together with PAR1 to lysosomes for degradation. This PAR1-induced lysosomal degradation of Src may be specific for the termination of PAR1-mediated endosomal Src signalling.

Acknowledgements

Author contributions

C-CT performed the experiments, analysed the data and wrote the manuscript. F-TK designed and performed the experiments. S-BL performed the experiments and helped to write the manuscript. Y-TC performed the experiments. H-WF conceived the study, supervised, designed and conducted the experiments, and wrote the manuscript. All the authors reviewed the manuscript.

References

1 Grand RJ, Turnell AS and Grabham PW (1996) Cellular consequences of thrombin-receptor activation. *Biochem J* **313** (Pt 2), 353–368.

2 Chen D and Dorling A (2009) Critical roles for thrombin in acute and chronic inflammation. *J Thromb Haemost* **7** (Suppl 1), 122–126.

3 Siller-Matula JM, Schwameis M, Blann A, Mannhalter C and Jilma B (2011) Thrombin as a multi-functional enzyme. Focus on in vitro and in vivo effects. *Thromb Haemost* **106**, 1020–1033.

4 Vu TK, Hung DT, Wheaton VI and Coughlin SR (1991) Molecular cloning of a functional thrombin receptor reveals a novel proteolytic mechanism of receptor activation. *Cell* **64**, 1057–1068.

5 Coughlin SR (1999) How the protease thrombin talks to cells. *Proc Natl Acad Sci USA* **96**, 11023–11027.

6 Vassallo RR Jr, Kieber-Emmons T, Cichowski K and Brass LF (1992) Structure-function relationships in the activation of platelet thrombin receptors by receptor-derived peptides. *J Biol Chem* **267**, 6081–6085.

7 Scarborough RM, Naughton MA, Teng W, Hung DT, Rose J, Vu TK, Wheaton VI, Turck CW and Coughlin SR (1992) Tethered ligand agonist peptides. Structural requirements for thrombin receptor activation reveal mechanism of proteolytic unmasking of agonist function. *J Biol Chem* **267**, 13146–13149.

8 Macfarlane SR, Seatter MJ, Kanke T, Hunter GD and Plevin R (2001) Proteinase-activated receptors. *Pharmacol Rev* **53**, 245–282.

9 Tiruppathi C, Yan W, Sandoval R, Naqvi T, Pronin AN, Benovic JL and Malik AB (2000) G protein-coupled receptor kinase-5 regulates thrombin-activated signaling in endothelial cells. *Proc Natl Acad Sci USA* **97**, 7440–7445.

10 Ishii K, Chen J, Ishii M, Koch WJ, Freedman NJ, Lefkowitz RJ and Coughlin SR (1994) Inhibition of thrombin receptor signaling by a G-protein coupled receptor kinase. Functional specificity among G-protein coupled receptor kinases. *J Biol Chem* **269**, 1125–1130.

11 Paing MM, Stutts AB, Kohout TA, Lefkowitz RJ and Trejo J (2002) beta -Arrestins regulate protease-activated receptor-1 desensitization but not internalization or Down-regulation. *J Biol Chem* **277**, 1292–1300.

12 Chen CH, Paing MM and Trejo J (2004) Termination of protease-activated receptor-1 signaling by beta-arrestins is independent of receptor phosphorylation. *J Biol Chem* **279**, 10020–10031.

13 Hoxie JA, Ahuja M, Belmonte E, Pizarro S, Parton R and Brass LF (1993) Internalization and recycling of activated thrombin receptors. *J Biol Chem* **268**, 13756–13763.

14 Hein L, Ishii K, Coughlin SR and Kobilka BK (1994) Intracellular targeting and trafficking of thrombin receptors. A novel mechanism for resensitization of a G protein-coupled receptor. *J Biol Chem* **269**, 27719–27726.

15 Trejo J, Hammes SR and Coughlin SR (1998) Termination of signaling by protease-activated receptor-1 is linked to lysosomal sorting. *Proc Natl Acad Sci USA* **95**, 13698–13702.

16 Trejo J, Altschuler Y, Fu HW, Mostov KE and Coughlin SR (2000) Protease-activated receptor-1 down-regulation: a mutant HeLa cell line suggests novel requirements for PAR1 phosphorylation and recruitment to clathrin-coated pits. *J Biol Chem* **275**, 31255–31265.

17 Kuo FT, Lu TL and Fu HW (2006) Opposing effects of beta-arrestin1 and beta-arrestin2 on activation and degradation of Src induced by protease-activated receptor 1. *Cell Signal* **18**, 1914–1923.

18 Goel R, Phillips-Mason PJ, Raben DM and Baldassare JJ (2002) alpha-Thrombin induces rapid and sustained Akt phosphorylation by beta-arrestin1-dependent and -independent mechanisms, and only the sustained Akt phosphorylation is essential for G1 phase progression. *J Biol Chem* **277**, 18640–18648.

19 Thomas SM and Brugge JS (1997) Cellular functions regulated by Src family kinases. *Annu Rev Cell Dev Biol* **13**, 513–609.

20 Luttrell DK and Luttrell LM (2004) Not so strange bedfellows: G-protein-coupled receptors and Src family kinases. *Oncogene* **23**, 7969–7978.

21 Roskoski R Jr (2004) Src protein-tyrosine kinase structure and regulation. *Biochem Biophys Res Commun* **324**, 1155–1164.

22 Ma YC, Huang J, Ali S, Lowry W and Huang XY (2000) Src tyrosine kinase is a novel direct effector of G proteins. *Cell* **102**, 635–646.

23 Luttrell LM, Ferguson SS, Daaka Y, Miller WE, Maudsley S, Della Rocca GJ, Lin F, Kawakatsu H, Owada K, Luttrell DK *et al.* (1999) Beta-arrestin-dependent formation of beta2 adrenergic receptor-Src protein kinase complexes. *Science* **283**, 655–661.

24 Miller WE, Maudsley S, Ahn S, Khan KD, Luttrell LM and Lefkowitz RJ (2000) beta-arrestin1 interacts with the catalytic domain of the tyrosine kinase c-SRC. Role of beta-arrestin1-dependent targeting of c-SRC in receptor endocytosis. *J Biol Chem* **275**, 11312–11319.

25 Harris KF, Shoji I, Cooper EM, Kumar S, Oda H and Howley PM (1999) Ubiquitin-mediated degradation of active Src tyrosine kinase. *Proc Natl Acad Sci USA* **96**, 13738–13743.

26 Hakak Y and Martin GS (1999) Ubiquitin-dependent degradation of active Src. *Curr Biol* **9**, 1039–1042.

27 Lu TL, Kuo FT, Lu TJ, Hsu CY and Fu HW (2006) Negative regulation of protease-activated receptor 1-induced Src kinase activity by the association of phosphocaveolin-1 with Csk. *Cell Signal* **18**, 1977–1987.

28 Chen YH, Pouyssegur J, Courtneidge SA and Van Obberghen-Schilling E (1994) Activation of Src family kinase activity by the G protein-coupled thrombin receptor in growth-responsive fibroblasts. *J Biol Chem* **269**, 27372–27377.

29 Yin YJ, Salah Z, Maoz M, Even Ram SC, Ochayon S, Neufeld G, Katzav S and Bar-Shavit R (2003) Oncogenic transformation induces tumor angiogenesis: a role for PAR1 activation. *FASEB J* **17**, 163–174.

30 Lin CH, Cheng HW, Hsu MJ, Chen MC, Lin CC and Chen BC (2006) c-Src mediates thrombin-induced NF-kappaB activation and IL-8/CXCL8 expression in lung epithelial cells. *J Immunol* **177**, 3427–3438.

31 Chiu YC, Fong YC, Lai CH, Hung CH, Hsu HC, Lee TS, Yang RS, Fu WM and Tang CH (2008) Thrombin-induced IL-6 production in human synovial fibroblasts is mediated by PAR1, phospholipase C, protein kinase C alpha, c-Src, NF-kappa B and p300 pathway. *Mol Immunol* **45**, 1587–1599.

32 van der Bliek AM, Redelmeier TE, Damke H, Tisdale EJ, Meyerowitz EM and Schmid SL (1993) Mutations in human dynamin block an intermediate stage in coated vesicle formation. *J Cell Biol* **122**, 553–563.

33 Bishop N and Woodman P (2000) ATPase-defective mammalian VPS4 localizes to aberrant endosomes and impairs cholesterol trafficking. *Mol Biol Cell* **11**, 227–239.

34 Hong ZW, Yang YC, Pan T, Tzeng HF and Fu HW (2017) Differential effects of DEAE negative mode chromatography and gel-filtration chromatography on the charge status of *Helicobacter pylori* neutrophil-activating protein. *PLoS One* **12**, e0173632.

35 Dores MR, Chen B, Lin H, Soh UJ, Paing MM, Montagne WA, Meerloo T and Trejo J (2012) ALIX binds a YPX(3)L motif of the GPCR PAR1 and mediates ubiquitin-independent ESCRT-III/MVB sorting. *J Cell Biol* **197**, 407–419.

36 Altschuler Y, Barbas SM, Terlecky LJ, Tang K, Hardy S, Mostov KE and Schmid SL (1998) Redundant and distinct functions for dynamin-1 and dynamin-2 isoforms. *J Cell Biol* **143**, 1871–1881.

37 Pilecka I, Banach-Orlowska M and Miaczynska M (2007) Nuclear functions of endocytic proteins. *Eur J Cell Biol* **86**, 533–547.

38 Ahn S, Maudsley S, Luttrell LM, Lefkowitz RJ and Daaka Y (1999) Src-mediated tyrosine phosphorylation of dynamin is required for beta2-adrenergic receptor internalization and mitogen-activated protein kinase signaling. *J Biol Chem* **274**, 1185–1188.

39 Ahn S, Kim J, Lucaveche CL, Reedy MC, Luttrell LM, Lefkowitz RJ and Daaka Y (2002) Src-dependent tyrosine phosphorylation regulates dynamin self-assembly and ligand-induced endocytosis of the epidermal growth factor receptor. *J Biol Chem* **277**, 26642–26651.

40 Kim M, Tezuka T, Tanaka K and Yamamoto T (2004) Cbl-c suppresses v-Src-induced transformation through ubiquitin-dependent protein degradation. *Oncogene* **23**, 1645–1655.

41 Wolfe BL, Marchese A and Trejo J (2007) Ubiquitination differentially regulates clathrin-dependent internalization of protease-activated receptor-1. *J Cell Biol* **177**, 905–916.

42 Tu C, Ortega-Cava CF, Winograd P, Stanton MJ, Reddi AL, Dodge I, Arya R, Dimri M, Clubb RJ, Naramura M *et al.* (2010) Endosomal-sorting complexes required for transport (ESCRT) pathway-dependent endosomal traffic regulates the localization of active Src at focal adhesions. *Proc Natl Acad Sci USA* **107**, 16107–16112.

43 Reinecke J and Caplan S (2014) Endocytosis and the Src family of non-receptor tyrosine kinases. *Biomol Concepts* **5**, 143–155.

44 Kang DS, Tian X and Benovic JL (2014) Role of beta-arrestins and arrestin domain-containing proteins in G protein-coupled receptor trafficking. *Curr Opin Cell Biol* **27**, 63–71.

45 Cao H, Chen J, Krueger EW and McNiven MA (2010) SRC-mediated phosphorylation of dynamin and cortactin regulates the "constitutive" endocytosis of transferrin. *Mol Cell Biol* **30**, 781–792.

46 Wilde A, Beattie EC, Lem L, Riethof DA, Liu SH, Mobley WC, Soriano P and Brodsky FM (1999) EGF receptor signaling stimulates SRC kinase phosphorylation of clathrin, influencing clathrin redistribution and EGF uptake. *Cell* **96**, 677–687.

47 Fessart D, Simaan M, Zimmerman B, Comeau J, Hamdan FF, Wiseman PW, Bouvier M and Laporte SA (2007) Src-dependent phosphorylation of beta2-adaptin dissociates the beta-arrestin-AP-2 complex. *J Cell Sci* **120**, 1723–1732.

48 Zimmerman B, Simaan M, Lee MH, Luttrell LM and Laporte SA (2009) c-Src-mediated phosphorylation of AP-2 reveals a general mechanism for receptors internalizing through the clathrin pathway. *Cell Signal* **21**, 103–110.

49 Lin X, Zhang J, Chen L, Chen Y, Xu X, Hong W and Wang T (2017) Tyrosine phosphorylation of Rab7 by Src kinase. *Cell Signal* **35**, 84–94.

50 Hung DT, Wong YH, Vu TK and Coughlin SR (1992) The cloned platelet thrombin receptor couples to at least two distinct effectors to stimulate phosphoinositide hydrolysis and inhibit adenylyl cyclase. *J Biol Chem* **267**, 20831–20834.

Supporting information

Additional supporting information may be found online in the Supporting Information section at the end of the article.

Fig. S1. Src acts as a main upstream molecule of ERK1/2 in HEK293 cells after PAR1 activation.

Fig. S2. Activated PAR1 co-localizes with clathrin in the membrane patch of HEK293 cells.